Measurement of $D^+ \to K_S^0 K^+$ and $D_s^+ \to K_S^0 \pi^+$ branching ratios

E. Won,[14] B. R. Ko,[14] H. Aihara,[41] K. Arinstein,[1,30] V. Aulchenko,[1,30] T. Aushev,[16,11] A. M. Bakich,[37] V. Balagura,[11]
E. Barberio,[20] A. Bay,[16] K. Belous,[10] V. Bhardwaj,[32] M. Bischofberger,[22] A. Bondar,[1,30] A. Bozek,[26] M. Bračko,[18,12]
T. E. Browder,[6] P. Chang,[25] A. Chen,[23] P. Chen,[25] B. G. Cheon,[5] C.-C. Chiang,[25] I.-S. Cho,[45] Y. Choi,[36] J. Dalseno,[19,39]
A. Das,[38] S. Eidelman,[1,30] D. Epifanov,[1,30] S. Esen,[2] N. Gabyshev,[1,30] A. Garmash,[1,30] B. Golob,[17,12] H. Ha,[14] J. Haba,[7]
B.-Y. Han,[14] Y. Hasegawa,[35] K. Hayasaka,[21] H. Hayashii,[22] Y. Hoshi,[40] W.-S. Hou,[25] Y. B. Hsiung,[25] H. J. Hyun,[15]
T. Iijima,[21] K. Inami,[21] R. Itoh,[7] M. Iwasaki,[41] Y. Iwasaki,[7] N. J. Joshi,[38] T. Julius,[20] J. H. Kang,[45] N. Katayama,[7]
T. Kawasaki,[28] C. Kiesling,[19] H. J. Kim,[15] H. O. Kim,[15] J. H. Kim,[36] S. K. Kim,[34] Y. I. Kim,[15] Y. J. Kim,[4] S. Korpar,[18,12]
P. Krokovny,[7] T. Kumita,[42] A. Kuzmin,[1,30] Y.-J. Kwon,[45] S.-H. Kyeong,[45] J. S. Lange,[3] M. J. Lee,[34] S.-H. Lee,[14] J. Li,[6]
C. Liu,[33] Y. Liu,[21] D. Liventsev,[11] R. Louvot,[16] F. Mandl,[9] S. McOnie,[37] H. Miyata,[28] Y. Miyazaki,[21] T. Mori,[21]
E. Nakano,[31] M. Nakao,[7] H. Nakazawa,[23] Z. Natkaniec,[26] S. Nishida,[7] O. Nitoh,[43] T. Ohshima,[21] S. Okuno,[13] P. Pakhlov,[11]
G. Pakhlova,[11] H. Palka,[26] C. W. Park,[36] H. Park,[15] H. K. Park,[15] K. S. Park,[36] L. S. Peak,[37] R. Pestotnik,[12] M. Petrič,[12]
L. E. Piilonen,[44] A. Poluektov,[1,30] S. Ryu,[34] H. Sahoo,[6] Y. Sakai,[7] O. Schneider,[16] C. Schwanda,[9] M. E. Sevior,[20]
M. Shapkin,[10] V. Shebalin,[1,30] J.-G. Shiu,[25] B. Shwartz,[1,30] P. Smerkol,[12] A. Sokolov,[10] E. Solovieva,[11] S. Stanič,[29]
M. Starič,[12] T. Sumiyoshi,[42] G. N. Taylor,[20] Y. Teramoto,[31] K. Trabelsi,[7] S. Uehara,[7] Y. Unno,[5] S. Uno,[7] P. Urquijo,[20]
Y. Usov,[1,30] G. Varner,[6] K. E. Varvell,[37] K. Vervink,[16] A. Vinokurova,[1,30] C. H. Wang,[24] P. Wang,[8] Y. Watanabe,[13]
R. Wedd,[20] B. D. Yabsley,[37] Y. Yamashita,[27] M. Yamauchi,[7] C. C. Zhang,[8] Z. P. Zhang,[33] V. Zhilich,[1,30] V. Zhulanov,[1,30]
T. Zivko,[12] A. Zupanc,[12] and O. Zyukova[1,30]

(The Belle Collaboration)

[1]*Budker Institute of Nuclear Physics, Novosibirsk*
[2]*University of Cincinnati, Cincinnati, Ohio 45221*
[3]*Justus-Liebig-Universität Gießen, Gießen*
[4]*The Graduate University for Advanced Studies, Hayama*
[5]*Hanyang University, Seoul*
[6]*University of Hawaii, Honolulu, Hawaii 96822*
[7]*High Energy Accelerator Research Organization (KEK), Tsukuba*
[8]*Institute of High Energy Physics, Chinese Academy of Sciences, Beijing*
[9]*Institute of High Energy Physics, Vienna*
[10]*Institute of High Energy Physics, Protvino*
[11]*Institute for Theoretical and Experimental Physics, Moscow*
[12]*J. Stefan Institute, Ljubljana*
[13]*Kanagawa University, Yokohama*
[14]*Korea University, Seoul*
[15]*Kyungpook National University, Taegu*
[16]*École Polytechnique Fédérale de Lausanne (EPFL), Lausanne*
[17]*Faculty of Mathematics and Physics, University of Ljubljana, Ljubljana*
[18]*University of Maribor, Maribor*
[19]*Max-Planck-Institut für Physik, München*
[20]*University of Melbourne, School of Physics, Victoria 3010*
[21]*Nagoya University, Nagoya*
[22]*Nara Women's University, Nara*
[23]*National Central University, Chung-li*
[24]*National United University, Miao Li*
[25]*Department of Physics, National Taiwan University, Taipei*
[26]*H. Niewodniczanski Institute of Nuclear Physics, Krakow*
[27]*Nippon Dental University, Niigata*
[28]*Niigata University, Niigata*
[29]*University of Nova Gorica, Nova Gorica*
[30]*Novosibirsk State University, Novosibirsk*
[31]*Osaka City University, Osaka*
[32]*Panjab University, Chandigarh*
[33]*University of Science and Technology of China, Hefei*
[34]*Seoul National University, Seoul*
[35]*Shinshu University, Nagano*

^{36}*Sungkyunkwan University, Suwon*

^{37}*School of Physics, University of Sydney, NSW 2006*

^{38}*Tata Institute of Fundamental Research, Mumbai*

^{39}*Excellence Cluster Universe, Technische Universität München, Garching*

^{40}*Tohoku Gakuin University, Tagajo*

^{41}*Department of Physics, University of Tokyo, Tokyo*

^{42}*Tokyo Metropolitan University, Tokyo*

^{43}*Tokyo University of Agriculture and Technology, Tokyo*

^{44}*IPNAS, Virginia Polytechnic Institute and State University, Blacksburg, Virginia 24061*

^{45}*Yonsei University, Seoul*

We report an improved measurement of $D^+ \to K_S^0 K^+$ and $D_s^+ \to K_S^0 \pi^+$ branching ratios using 605 fb^{-1} of data collected with the Belle detector at the KEKB asymmetric-energy e^+e^- collider. The measured branching ratios with respect to the Cabibbo-favored modes are $\mathcal{B}(D^+ \to K_S^0 K^+)/\mathcal{B}(D^+ \to K_S^0 \pi^+) = 0.1899 \pm 0.0011 \pm 0.0022$ and $\mathcal{B}(D_s^+ \to K_S^0 \pi^+)/\mathcal{B}(D_s^+ \to K_S^0 K^+) = 0.0803 \pm 0.0024 \pm 0.0019$ where the first uncertainties are statistical and the second are systematic.

Decays of charmed mesons play an important role in understanding the sources of SU(3) flavor symmetry breaking [1]. Such a breaking can originate from strong final-state interactions or interference between amplitudes with the same final state. In particular, $D^+ \to \bar{K}^0 K^+$ and $D_s^+ \to K^0 \pi^+$ [2] are Cabibbo-suppressed (CS) decays that involve color-favored tree, annihilation, and penguin diagrams. For D^+ decays, the branching ratio $\mathcal{B}(D^+ \to \bar{K}^0 K^+)/\mathcal{B}(D^+ \to \bar{K}^0 \pi^+)$ deviates from the naive $\tan^2\theta_C$ expectation [3], due to the destructive interference between color-favored and color-suppressed amplitudes in $D^+ \to \bar{K}^0 \pi^+$ [4]. However, converting experimental measurements of D decays that include K_S^0 branching ratios to those involving K^0 or $\bar{K}^0$ is not straightforward due to the interference between the doubly Cabibbo-suppressed and Cabibbo-favored (CF) decay modes where the interference phase is unknown [5,6]. In D_s^+ decays to $\bar{K}^0 K^+$ and $K^0 \pi^+$ final states, the ratio of the CS decay to the corresponding CF decay may be larger than $\tan^2\theta_C$, since the tree diagram for $D_s^+ \to \bar{K}^0 K^+$ is CF but color suppressed. Precise measurements of branching ratios for CS and CF charmed meson decay modes can thus improve the understanding of the underlying dynamics of these decays. In this paper, we report improved measurements of the $D^+ \to K_S^0 K^+$ and $D_s^+ \to K_S^0 \pi^+$ branching ratios with respect to the corresponding CF modes, $D^+ \to K_S^0 \pi^+$ and $D_s^+ \to K_S^0 K^+$, respectively.

The results are based on a data sample of 605 fb^{-1} recorded at the $\Upsilon(4S)$ resonance with the Belle detector at the KEKB asymmetric-energy e^+e^- collider [7]. An additional data sample with about 10% of this integrated luminosity recorded 60 MeV below the $\Upsilon(4S)$ was used for the optimization of the selection criteria (off-resonance sample). The Belle detector is a large-solid-angle magnetic spectrometer that consists of a silicon vertex detector, a 50-layer central drift chamber, an array of aerogel threshold Cherenkov counters, a barrel-like arrangement of time-of-flight scintillation counters, and an electromagnetic calorimeter comprised of CsI(Tl) crystals located inside a superconducting solenoid coil that provides a 1.5 T magnetic field. An iron flux return located outside the coil is instrumented to detect K_L^0 mesons and to identify muons. The detector is described in detail elsewhere [8].

We require that the charged tracks originate from the vicinity of the interaction point (IP) with the impact parameters in the beam direction (z axis) and perpendicular to it of less than 4 cm and 2 cm, respectively. All charged tracks except those originating from K_S^0 decays are required to have at least two associated hits in the silicon vertex detector, both in the z and radial directions, to assure good spatial resolution on the D mesons' decay vertices. Charged tracks are identified as pions or kaons by requiring the ratio of particle identification likelihoods, $\mathcal{L}_K/(\mathcal{L}_K + \mathcal{L}_\pi)$, constructed using information from the central drift chamber, time-of-flight scintillation counters, and aerogel threshold Cherenkov counters, be larger or smaller than 0.6, respectively. For both kaons and pions, the efficiencies and misidentification probabilities are 86% and 10%, respectively.

Pairs of oppositely charged tracks that have an invariant mass within 30 MeV/c^2 of the nominal K_S^0 mass are used to reconstruct $K_S^0 \to \pi^+\pi^-$ decays. The distance of the closest approach of the candidate charged tracks to the IP in the plane perpendicular to the z axis is required to be larger than 0.02 cm for high-momentum (> 1.5 GeV/c) K_S^0 candidates and 0.03 cm for those with momentum less than 1.5 GeV/c. The $\pi^+\pi^-$ vertex is required to be displaced from the IP by a minimum transverse distance of 0.22 cm for high-momentum candidates and 0.08 cm for the remaining candidates. The mismatch in the z direction at the K_S^0 vertex point for the $\pi^+\pi^-$ tracks must be less than 2.4 cm for high-momentum candidates and 1.8 cm for the remaining candidates. The direction of the pion pair momentum must also agree with the direction of the vertex

point from the IP to within 0.03 rad for high-momentum candidates and to within 0.1 rad for the remaining candidates.

These two sets of criteria in two different momentum ranges are implemented to maximize $\mathcal{N}_S / \sqrt{\mathcal{N}_S + \mathcal{N}_B}$, where $\mathcal{N}_S$ and $\mathcal{N}_B$ are the number of signal K^0_S's and the number of combinatorial background events, respectively. Finally, the $\pi^+ \pi^-$ pair forming a K^0_S candidate is required to have an invariant mass within ± 9 MeV/c^2 of the nominal K^0_S mass [3].

D^+ and D^+_s candidates are reconstructed using a K^0_S candidate and either a charged pion or kaon candidate. The decay vertex is formed by fitting the K^0_S and the track to a common vertex and requiring a confidence level greater than 0.1%. In order to remove peaking backgrounds from the $D^+_{(s)} \to \pi^+ \pi^+ \pi^-$ and $K^+ \pi^+ \pi^-$ decay modes, we compute the reduced χ^2 of the vertex assuming that two pions from the K^0_S and the charm daughter track arise from a single vertex. We require the reduced χ^2 to be greater than 10.

To remove D^+ and D^+_s mesons produced in B meson decays, we require the charmed meson momentum calculated in the center-of-mass frame to be greater than 2.6 GeV/c. At this stage, reconstruction efficiencies are 16.6% for the D^+ and 18.0% for the D^+_s in the $K^0_S K^+$ final state, and 20.6% for the D^+ and 22.4% for the D^+_s in the $K^0_S \pi^+$ final state.

Highly asymmetrical $K^0_S h^+$ pairs that have invariant mass close to the $D^+_{(s)}$ mass region are more likely to be background than signal. The asymmetry, $\mathcal{A} \equiv |p_{K^0_S} - p_{h^+}| / |p_{K^0_S} + p_{h^+}|$, where each momenta is calculated in the laboratory frame and h^+ refers to either a K^+ or π^+, is used to reject background candidates. The $\mathcal{A}$ requirement is optimized in both CS modes by maximizing $\mathcal{N}_S / \sigma_{\mathcal{N}_S}$, where $\mathcal{N}_S$ is the signal yield and $\sigma_{\mathcal{N}_S}$ is the statistical uncertainty in $\mathcal{N}_S$ from the fit to the off-resonance data sample. The asymmetry is required to be less than 0.6 for both decay modes. After this final requirement, we find 10% and 35% improvements in $\mathcal{N}_S / \sigma_{\mathcal{N}_S}$ for CS decay modes of the D^+ and D^+_s, respectively.

Since there are differences in the mass distributions between the data and Monte Carlo (MC) simulated [9] samples, we tune the large MC samples of generic continuum and $B\bar{B}$ decays, intended mainly for the accurate parametrization of the peaking background under the signal. This background is a consequence of particle misidentification and will be discussed in more detail later. The tuning procedure is as follows: the π^+ (K^+) momentum scale and resolution are tuned with the $D^0 \to \pi^+ \pi^-$ ($D^0 \to K^+ K^-$) data sample. For the K^0_S momentum scale and resolution tuning, the $D^+ \to K^0_S \pi^+$ data sample is used. The tuning method is validated by comparing simulated and real data in the $K^0_S K^+$ final state. The four signal decay modes are simulated and the results of the tuning are also applied to them.

In the branching ratio measurements, there is a peaking background due to particle misidentification. In the $D^+_s \to K^0_S K^+$ mass region, there is a peaking structure from $D^+ \to K^0_S \pi^+$ decays when a π^+ is misidentified as a K^+. A similar peaking structure in the $D^+ \to K^0_S \pi^+$ mass region appears due to misidentification in $D^+_s \to K^0_S K^+$ decays. The shapes and the yields of these peaking backgrounds are obtained from the tuned simulation samples and are used as the probability density functions (PDF) for the peaking backgrounds. The simulated shape and normalization of the peaking backgrounds are checked by comparing the invariant mass distributions of selected $K^0_S K^+$ ($K^0_S \pi^+$) pairs with the K^+ (π^+) mass assignment changed to a π^+ (K^+) mass assignment. The comparison shows that the simulated peaking background of the tuned sample correctly describes these components and that misidentification is indeed the only contribution above the structureless combinatorial background. Uncertainties in the misidentification probabilities are considered as a source of systematic uncertainty.

The $K^0_S K^+$ and $K^0_S \pi^+$ invariant mass distributions after the final selections are shown in Figs. 1 and 2 together with the signal and background parametrizations. Clear signals for CF and CS decays are observed in both distributions. The $K^0_S K^+$ and $K^0_S \pi^+$ invariant mass distributions are fitted using a binned maximum likelihood method. In all cases the signal PDF is parametrized using two Gaussians with a common mean value. For $D^+_s \to K^0_S \pi^+$, we fix the ratio of widths and the fractional yields in the two Gaussians because of the low statistics. The values of the ratio and the fraction of the broader Gaussian are obtained from the fit to the $D^+ \to K^0_S \pi^+$ mode and are consistent with the
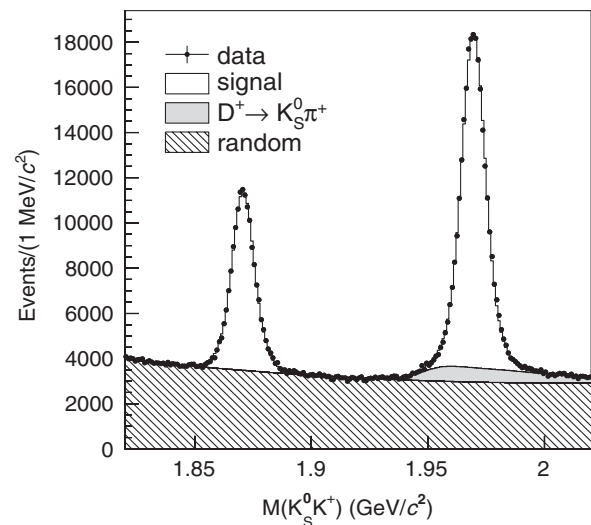

FIG. 1. Invariant mass distribution of selected $K^0_S K^+$ pairs. Points with error bars show the data and histograms show the results of the fits described in the text. Signal, $D^+ \to K^0_S \pi^+$ background, and random combinatorial background components are also shown.

FIG. 2. Invariant mass distribution of selected $K_S^0 \pi^+$ pairs. Points with error bars show the data and histograms show the results of the fits described in the text. Signal, $D_s^+ \rightarrow K_S^0 K^+$ background, and random combinatorial background components are also shown. The inset is an enlarged view of the D_s^+ region.
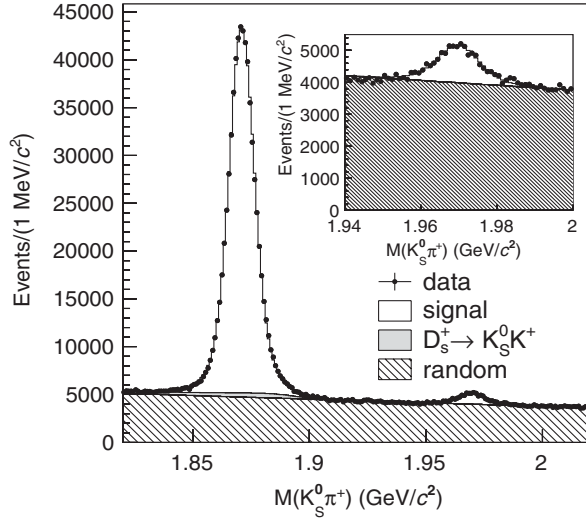
results of fits to the MC simulated signal. The reduced χ^2 values of the fits are 1.8 and 2.3 for the $K_S^0 K^+$ and $K_S^0 \pi^+$ final states, respectively. The normalization of the mass distributions of the misidentified K/π backgrounds are fixed to the values obtained from tuned simulation samples. Combinatorial background PDFs are parametrized using second and first-order polynomials for the $K_S^0 K^+$ and $K_S^0 \pi^+$ final states, respectively. All the fit parameters are allowed to float except for the $D_s^+ \rightarrow K_S^0 \pi^+$ signal PDF parameters and the yield and the normalization of the misidentified backgrounds. Table I summarizes the extracted signal yields from the fits to data and corresponding signal efficiencies from the simulated signal samples where final-state radiation has been included [10].

Various contributions to the systematic uncertainties for the branching ratio measurements are summarized in Table II. Several sources of systematic uncertainty are reduced in ratio measurements due to the similar kinematics of CF and CS decays. Such sources include the tracking and asymmetry variable efficiency differences between simulated data and real data. However, the systematic uncertainty due to particle identification efficiency does

TABLE I. The extracted signal yields from the fits to data and corresponding signal efficiencies (ϵ) from the simulated events of signal modes. The uncertainties are statistical only.

Decay modes	Yields	ϵ (%)
$D^+ \rightarrow K_S^0 K^+$	$100\,855 \pm 561$	12.59 ± 0.01
$D_s^+ \rightarrow K_S^0 K^+$	$204\,093 \pm 768$	13.53 ± 0.01
$D^+ \rightarrow K_S^0 \pi^+$	$566\,285 \pm 1162$	14.19 ± 0.01
$D_s^+ \rightarrow K_S^0 \pi^+$	$17\,583 \pm 481$	15.35 ± 0.01

TABLE II. Relative systematic uncertainties in percent, where $\sigma_{R(D^+)}$ and $\sigma_{R(D_s^+)}$ are systematic uncertainties for branching ratios of D^+ and D_s^+ decays. Sources include particle identification (PID), fit methods, peaking background, and the D_s^+ signal PDF.

Source	$\sigma_{R(D^+)}$ (%)	$\sigma_{R(D_s^+)}$ (%)
PID	0.90	0.90
Fit methods	0.74	2.00
Peaking background	0.16	0.62
D_s^+ signal PDF	$\cdots$	0.37
Total	1.18	2.31

not cancel. The particle identification efficiency differences between real data and simulated events are estimated independently using the decay $D^{*+} \rightarrow D^0 \pi^+$ followed by $D^0 \rightarrow K^- \pi^+$ and corrections from this estimate are applied to signal efficiencies in Table I. These corrections are 1.000 ± 0.007 and 0.946 ± 0.005 for K^+ and π^+ candidates, respectively. Uncertainties in the particle identification corrections are included in the systematics estimate and are found to be 0.90% of the measured ratios. In order to validate the entire analysis procedure, we fit large numbers of simulated samples of generic continuum and $B\bar{B}$ decays, and find no bias in the procedure within the statistical uncertainties of our measurements. We refit the data with various histogram binnings, different fit intervals, and different combinatorial background PDFs. We also refit the data in the D^+ and D_s^+ samples separately. We estimate 0.74% and 2.00% of the measured ratios as the systematic uncertainties due to variations in fit methods for the D^+ and D_s^+ modes, respectively. Particle identification and the associated normalizations of the K/π misidentified background yields in fits are also estimated using the measured misidentification rates and found to be 0.16% and 0.62% of the measured ratio for the D^+ and D_s^+ modes, respectively. Finally, systematic effects due to the extra constraints in the $D_s^+ \rightarrow K_S^0 \pi^+$ signal PDF are estimated by refitting the data allowing the fixed parameters to change within their 1 standard deviation uncertainties. This gives a negligible effect in D^+ decays but there is a systematic effect corresponding to 0.37% of the measured ratio in D_s^+ decay modes. Table II summarizes the systematic uncertainties in the branching ratio measurements.

With the signal efficiencies and the corrections due to particle identification efficiency differences, we find the branching ratios to be

$$R(D^+) \equiv \frac{\mathcal{B}(D^+ \rightarrow K_S^0 K^+)}{\mathcal{B}(D^+ \rightarrow K_S^0 \pi^+)}$$

$$= 0.1899 \pm 0.0011 \pm 0.0022,$$

$$R(D_s^+) \equiv \frac{\mathcal{B}(D_s^+ \rightarrow K_S^0 \pi^+)}{\mathcal{B}(D_s^+ \rightarrow K_S^0 K^+)} = 0.0803 \pm 0.0024 \pm 0.0019$$

TABLE III. Branching ratios for the D^+ and the D_s^+, and comparisons with previous measurements. The uncertainties shown combine the statistical and systematic uncertainties of our results.

Branching ratio	Belle exp.	World average [3]
$R(D^+)$	$(19.0 \pm 0.2)\%$	$(20.6 \pm 1.4)\%$
$R(D_s^+)$	$(8.0 \pm 0.3)\%$	$(8.4 \pm 0.9)\%$

where the first uncertainties are statistical and the second are systematic. These are the most precise measurements to date and are compared to the present world average values in Table III. Our measurement of $R(D^+)$ is in good agreement with previous measurements [3] and is larger than the naive expectation of $\tan^2\theta_C$, consistent with the expected destructive interference effect mentioned earlier. For D_s^+ decays, there is no such interference and $R(D_s^+)$ is found to be greater than $\tan^2\theta_C$ by more than 8 standard deviations, consistent with previous measurements [3]. This large deviation may be due to the color suppression of the main $D_s^+ \to K_S^0 K^+$ amplitude.

To conclude, using 605 fb^{-1} of data collected with the Belle detector at the KEKB asymmetric-energy e^+e^- collider we have measured the $D^+ \to K_S^0 K^+$ and $D_s^+ \to K_S^0 \pi^+$ branching ratios with respect to the corresponding Cabibbo-favored modes. The results are $\mathcal{B}(D^+ \to K_S^0 K^+)/\mathcal{B}(D^+ \to K_S^0 \pi^+) = 0.1899 \pm 0.0011 \pm 0.0022$ and $\mathcal{B}(D_s^+ \to K_S^0 \pi^+)/\mathcal{B}(D_s^+ \to K_S^0 K^+) = 0.0803 \pm 0.0024 \pm 0.0019$, where the first uncertainties are statistical and the second are systematic. Using the world average values of CF decay rates [3], we obtain the branching fractions $\mathcal{B}(D^+ \to K_S^0 K^+) = (2.75 \pm 0.08) \times 10^{-3}$ and $\mathcal{B}(D_s^+ \to K_S^0 \pi^+) = (1.20 \pm 0.09) \times 10^{-3}$ where the uncertainties are the sum in quadrature of statistical and systematic errors. These are consistent with the present world averages [3] and are the most precise measurements

to date. The ratio $\mathcal{B}(D^+ \to K_S^0 K^+)/\mathcal{B}(D_s^+ \to K_S^0 \pi^+) = 2.29 \pm 0.18$ may be due to SU(3) flavor breaking and/or different final-state interactions in D^+ and D_s^+ decays.

[1] B. Bhattacharya and J. L. Rosner, Phys. Rev. D **77**, 114020 (2008).

[2] Throughout this paper, the inclusion of the charge-conjugate decay mode is implied unless otherwise stated.

[3] C. Amsler *et al.* (Particle Data Group), Phys. Lett. B **667**, 1 (2008).

[4] B. Guberina, S. Nussinov, R. D. Peccei, and R. Rückl, Phys. Lett. **89B**, 111 (1979).

[5] I. I. Bigi and H. Yamamoto, Phys. Lett. B **349**, 363 (1995).

[6] M. Bishai *et al.* (CLEO Collaboration), Phys. Rev. Lett. **78**, 3261 (1997).

[7] S. Kurokawa and E. Kikutani, Nucl. Instrum. Methods Phys. Res., Sect. A **499**, 1 (2003), and other papers included in this volume.

[8] A. Abashian *et al.* (Belle Collaboration), Nucl. Instrum. Methods Phys. Res., Sect. A **479**, 117 (2002).

[9] $e^+e^- \to c\bar{c}$ events are generated with PYTHIA, T. Sjöstrand *et al.*, Comput. Phys. Commun. **135**, 238 (2001), and decay with EVTGEN (http://www.slac.stanford.edu/~lange/EvtGen); the detector response is simulated with GEANT 3.21, R. Brun *et al.*, CERN Report No. DD/EE/84-1, 1984.

[10] E. Richter-Was, Phys. Lett. B **303**, 163 (1993).